

## ELASTO-PLASTIC DYNAMIC RESPONSE OF REINFORCED CONCRETE NUCLEAR CONTAINMENT VESSEL WITH TENSION SOFTENING

B.K. Raghu Prasad and A.R. Gopalakrishnan

Indian Institute of Science, Bangalore, India

### ABSTRACT

In this paper, a study of elasto-plastic dynamic response of a reinforced concrete nuclear containment vessel due to El centro 1940 earthquake ground motion by Finite Element Method is presented. Shell elements with steel smeared are adopted. A method similar to initial stress method is used to include softening in dynamic analysis. Simplified von Mises criteria for yielding of concrete in compression are used while, cracking is modelled using bilinear softening law for concrete. Natural frequencies and time history responses of the structure at various stages of yielding and cracking are obtained to understand how the structure degrades in the nonlinear response.

### 1 INTRODUCTION

Softening has currently become a very interesting and challenging issue for researchers in the field of concrete structures. While softening has been more a challenge as a numerical technique (Balakrishnan and Murray) it is a basic conceptual issue in fracture mechanics of concrete. Nonlinear FEM like initial stress method (Zienkiewicz, Valliappan and King, 1969) have been in vogue for quite some time. But such methods do require modification when applied to concrete for the behaviour of concrete in tension is quite different from that in compression. Here infact one sees the importance of fracture mechanics. However, in this paper we will not deal with either a complete literature review of either non linear FEM or fracture mechanics of concrete. However, the relevant literature is briefly touched upon below.

Recent past has witnessed growing interest of many researchers in the field of nonlinear analysis of reinforced concrete structures. In early stages of investigation a reinforced concrete beam was idealized as a number of plane stress concrete elements and a few steel one dimensional elements connected through linkage elements (Ngo and Scordelis, 1967) to account for bond-slip with the cracks modelled as discrete. This was extended (Nilson, 1968) to include nonlinear material properties and a

bond-slip relationship. Then the simplified elasto-plastic behaviour of both concrete and steel (Valliappan and Doolan, 1972) using initial stress method was incorporated. In nonlinear finite element analysis of reinforced concrete structures (Suidan and Schnobrich 1973, Krishnamoorthy and Panneerselvam 1978) concrete is considered to behave nonlinearly in compression upto a yield surface. Beyond the yield surface concrete either is perfectly plastic or possess some non zero degraded stiffness. Concrete in tension is considered to behave linearly upto a limiting tensile strength,  $f_{ct}$ , at this point the concrete cracks and either cannot sustain any stresses in the direction normal to the cracking plane or else a softening is assumed with concrete stress decreasing with increased strain. In order to account for the steel reinforcement in stiffness calculation, reinforcing bars are modelled by three approaches (Chang Taniguchi and Chen 1987). These are (1) discrete model; (2) smeared model and (3) embedded model. In the discrete model the reinforcement is represented by a one dimensional bar elements superimposed on the two dimensional elements. In the smeared model, the overall constitutive relationship is simply evaluated by adding the material matrices for concrete and steel together by assuming the reinforcement distributed uniformly over the elements. In the embedded model (Colville and Abbasi, 1974) the stiffness of reinforcements is evaluated individually in the element in conjunction with isoparametric shape functions. This is used when reinforcements are sparsely located in the reinforcement concrete member. Also, their locations and orientations can be arbitrary. If bond-slip is disregarded the reinforcement bars may be modelled using smeared or embedded model.

Another model relatively more simple was proposed (Channakesava and Sundara Raja Iyengar, 1988) for a reinforced concrete structure. In the recent past there have been some more progress in this area. The works of (Chen and Saleeb, 1982 and Loo and Yang, 1991) are some examples. However, with all the above it is still not straight forward to include softening of a cracked element in a dynamic analysis as it becomes quite complicated numerically. Therefore, in this paper which is infact an improvement on the earlier paper by the author (Raghuprasad and Gopalakrishnan, 1991) softening has been included in dynamic analysis is an approach similar to the initial stress method.

## 2 ANALYSIS

The preliminary structure of a typical nuclear reactor vessel is idealized as a cylindrical shell, with a spherical cap as shown in Figure 1. Another shorter cylindrical shell is considered for the secondary portion. Real earthquake acceerograms of El centro, 1940 N-S component upto 8.0 seconds is considered as input. The well known SAP IV program (Bathe, Wilson and Peterson, 1974) has been used to perform dynamic analysis.

### 2.1 Finite element model for the nuclear containment vessel

The details of the finite element discretisation for half symmetry for the nuclear containment vessel are shown in Figures

2 (a), (b) and (c). The finite element discretisation consists of 291 nodes and 250 4-noded shell elements with six degrees of freedom per node. The model is fixed at the raft level. To account for the effect of steel reinforcement in stiffness calculations in the present study the smeared model for the reinforcement has been considered by taking 3% steel in both the direction of a typical concrete element. This model assumes perfect bond between steel and concrete. In the smeared model the overall constitutive relationship is evaluated by adding the material constitutive matrix for concrete and steel together.

Thus we have,  
 $[D] = [D_c] + \rho_s [D_s]$  in which (1)

$D$  = the composite material constitutive matrix for reinforced concrete

$D_c$  = the constitutive matrix of concrete

$\rho_s$  = volume ratio for the steel reinforcement

$D_s$  = the constitutive matrix for steel

$$[D]_c = E_c / (1 - \mu^2) \begin{bmatrix} 1 & \mu & 0 \\ \mu & 1 & 0 \\ 0 & 0 & (1 - \mu) / 2 \end{bmatrix} \quad (2)$$

$$[D]_s = \begin{bmatrix} E_s & 0 & 0 \\ 0 & E_s & 0 \\ 0 & 0 & 0 \end{bmatrix} \quad (3)$$

where  $E_c$  is the Young's modulus of concrete =  $5700 \sqrt{f_{ck}}$  N/mm<sup>2</sup>  
 $f_{ck}$  is the characteristics strength of concrete in N/mm<sup>2</sup>  
 $E_s$  is the Young's modulus of steel = 210000 N/mm<sup>2</sup>  
 $\mu$  is the Poisson's ratio of concrete = 0.15.

The grade of concrete is M20 and the corresponding tensile strength of concrete  $f_{ct} = 0.1 * f_{ck}$  where  $f_{ck} = 20$  N/mm<sup>2</sup>.

## 2.2 Failure criteria for concrete

The failure criteria proposed (Chen and Saleeb 1982) for plain concrete in tension related fractures is used in the present study. For crushing failure the simplified von Mises criterion is used. When the state of stress reaches a certain critical value the possible failure modes are described with the help of the so called failure zones illustrated in Figure 3 (a). In general, the material stiffness (Loo and Yang) is expressed as

$$[D_f] = \begin{bmatrix} K_1 E_c + \rho_s E_s & 0 & 0 & 0 \\ 0 & K_2 E_c + \rho_s E_s & 0 & 0 \\ 0 & 0 & 0 & 0 \\ 0 & 0 & 0 & K_3 G \end{bmatrix} \quad (4)$$

and  $G = E_c / 2(1 + \mu)$

where factors  $K_1$ ,  $K_2$  and  $K_3$  are given in Table 1 for the four

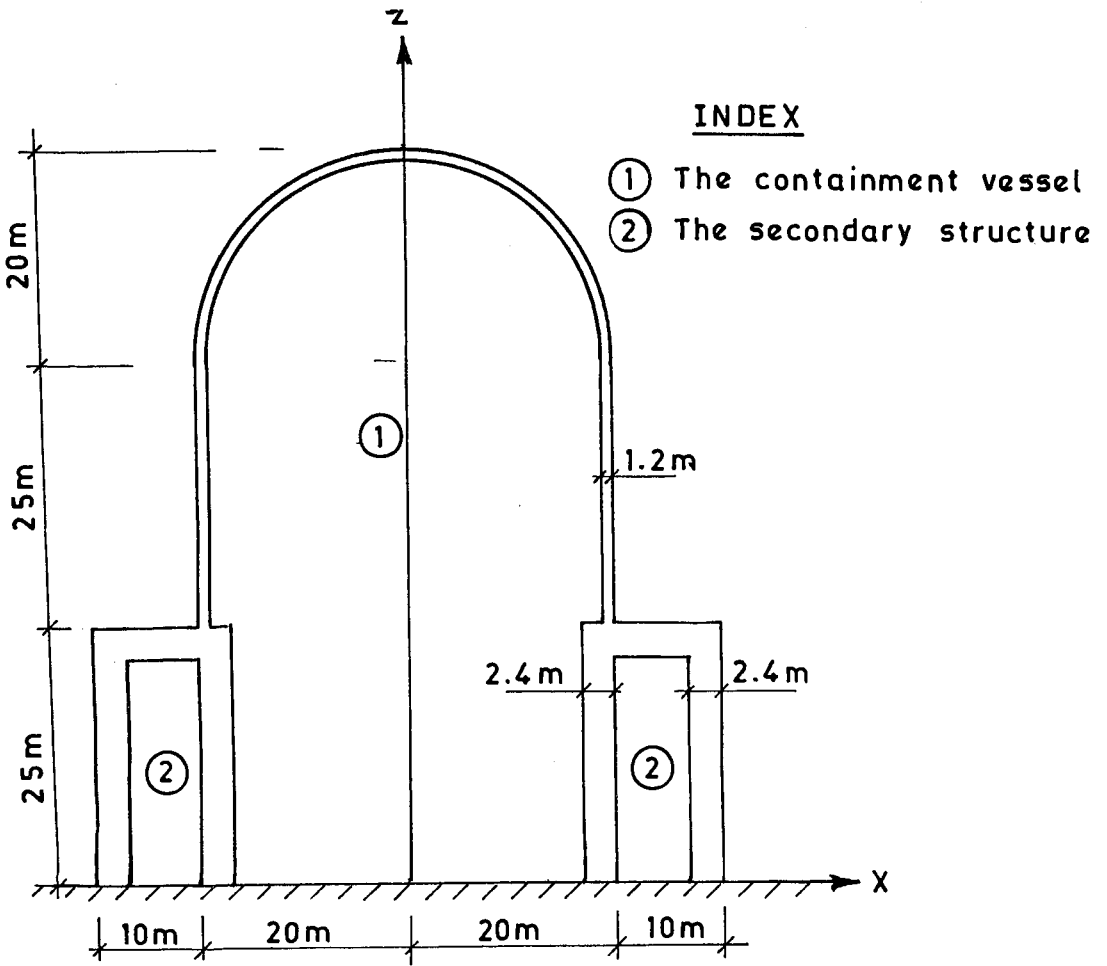


Fig.1 - The Nuclear Containment Vessel with the secondary structure

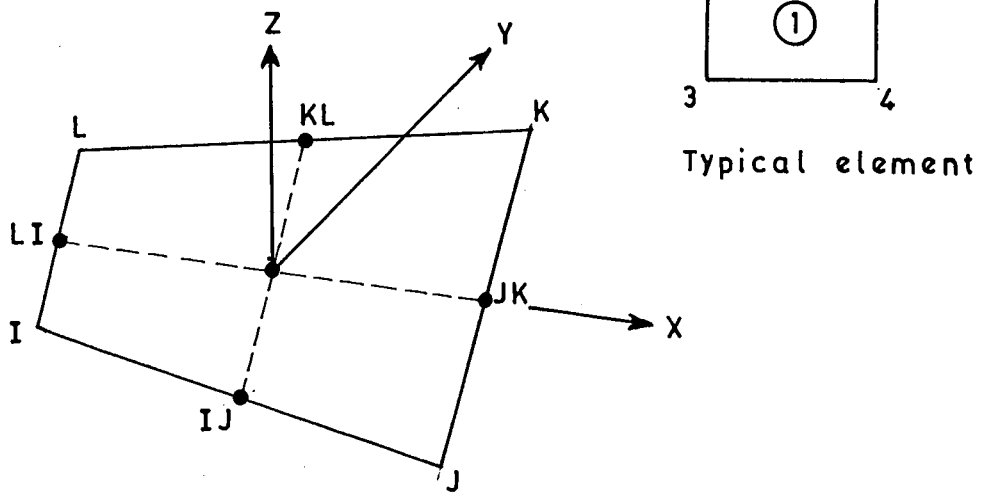


Fig. 2(b) Shell element coordinate axes

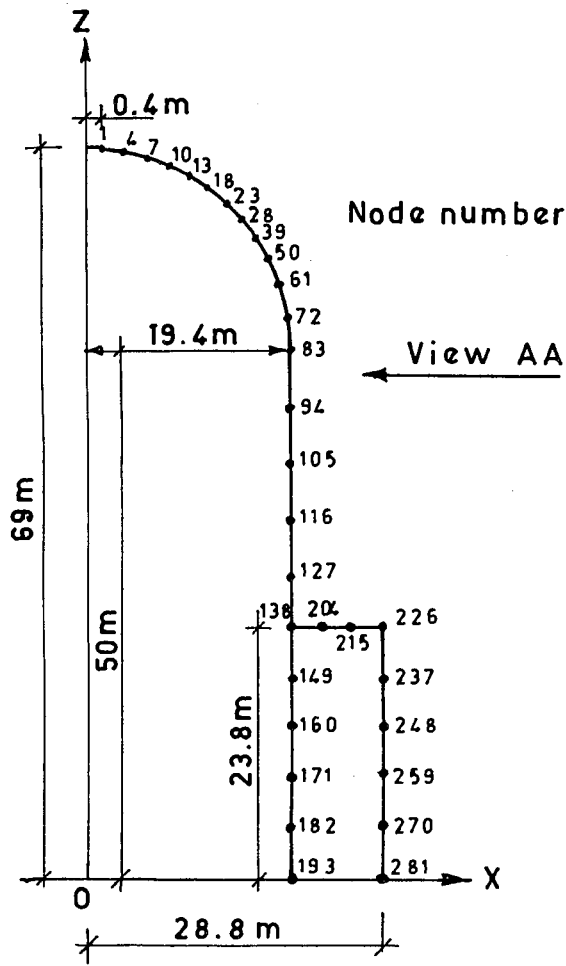


Fig. 2(a)- Finite element model for Nuclear Containment Vessel (Half symmetry FEM model)

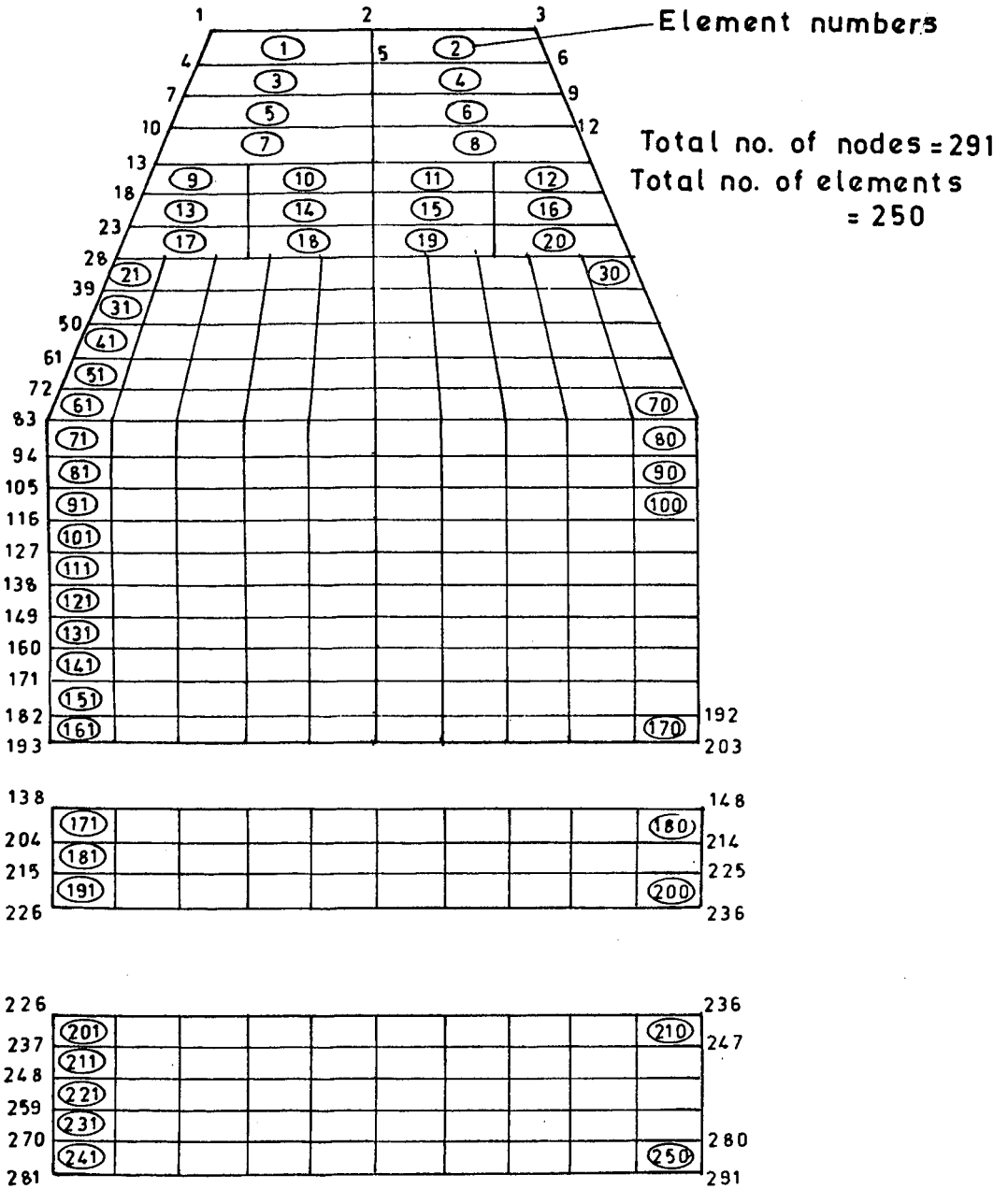


Fig. 2(c) - DEVELOPED VIEW AA SHOWING NODE NUMBERING AND ELEMENT NUMBERING

failure zones. In table 1,  $\phi$  is the stiffness-reduction factor and  $\beta$  is the crack surface interlock factor. In the present study, values for  $\phi$  are  $1.0 * E_c$ ,  $0.75 * E_c$ ,  $0.5 * E_c$ ,  $0.25 * E_c$ ,  $0.25 * E_c$  and  $0.0 * E_c$  and  $\beta$  is taken = 0.6 in all cases to study the effect of softening behaviour of concrete in tension.

Table 1 Factors in equation (4)

Zone	$K_1$	$K_2$	$K_3$
1	$\phi$	$\phi$	$\beta$
2	$\phi$	1	$\beta$
3	1	$\phi$	$\beta$
4	0	0	$\beta$

Zone 1 represents cracking of material in both the principal stress direction. In this case the state of stress is of the biaxial tension-tension type and both the principal stresses are beyond the tensile-failure envelope. In this situation, the material loses its tensile strength completely. Consequently, the stiffness reduction factor  $\phi$  has been considered various values to study the effect of softening behaviour of concrete instead of taking  $\phi = 0$ , which means that the stress in that direction is suddenly reduced to zero.

Cracking of material in one direction is characterized with state of stress is of the tension-compression type. The principal stress in  $\sigma_1$  direction exceeds the limiting value prescribed by the tensile failure surface for zone 2. In this case the material loses its tensile strength in the direction parallel to  $\sigma_1$ . For the case of a principal stress in the  $\sigma_2$  direction exceeding the limiting value defined by zone 3 tension - compression, the material loses its tensile strength in the direction parallel to  $\sigma_2$ . Finally, the crushing of material occurs when the state of stress level is beyond the simplified von Mises failure surface, defined by zone 4 under this condition the material also loses its strength completely. In this case  $\phi$  is taken as zero. In all the four failure modes the cracked concrete has been assumed to retain some shear stiffness due to interlocking and friction on the rough crack surface. This is accounted for by giving  $\beta$  a small value. In this study  $\beta$  is taken = 0.6.

### 2.3 Modelling of Tensile cracking of concrete

The cracking of concrete is the most significant factor as the concrete is weak in tension. In the present study the smeared crack model (Chen and Saleeb, 1982) is adopted. That is the cracked concrete is assumed to remain as a continuum rather than embodying a single discrete crack. The smeared crack is represented by an infinite number of parallel fissures across the cracked concrete element as shown in Figure 3 (b). Before cracking, the uncracked concrete is assumed to have the isotropic behaviour. In this case, the material stiffness matrix given in (1) is used. However, at the onset of cracking the orthotropic material properties exist and the matrix  $D_F$  relevant to the

various states can be obtained using (4). This is transformed to the global coordinate system using the transformation matrix [T] for the stiffness calculations.

$$[D] = [T]^T [D_f] [T] \quad (5)$$

$$\text{where } T = \begin{bmatrix} \cos^2 \theta & \sin^2 \theta & \cos \theta \sin \theta \\ \sin^2 \theta & \cos^2 \theta & -\cos \theta \sin \theta \\ -\sin 2\theta & \sin 2\theta & \cos^2 \theta - \sin^2 \theta \end{bmatrix} \quad (6)$$

and  $\theta$  angle of the crack direction.

#### 2.4 Modelling of compressive crushing of concrete

It is assumed that when crushing occurs under biaxial compression-compression stress state, the element is assumed to be smashed and all local stresses are released completely. It means that the material has lost its capacity to transmit any further load or to resist any further deformation. This is modelled using (4) with  $K_1 = K_2 = K_3 = \rho_s = 0$ .

#### 2.5 Dynamic Analysis

The equation of motion are (Biggs, 1964)

$$[M] \{\ddot{y}\} + [C] \{\dot{y}\} + [K] \{y\} = \{F(t)\} \quad (7)$$

where [M] is the mass matrix [C] is the damping matrix, [K] is the stiffness matrix and {F(t)} is the driving force. A uniform modal damping of 5% of the critical is considered. The solutions have been obtained by the mode superposition technique using five modes. A time step of  $T/10$  where T is the period of the fifth mode is taken.

In the analysis, the equation of motion (7) are solved in three stages. In the first stage the principal stresses obtained for each element from the dynamic analysis are checked with the failure criteria used for plain concrete as a material under biaxial stress state. The crushing and cracking of elements are traced. The cracked elements are then replaced with modified material constitutive matrix and the dynamic analysis is repeated to obtain the principal stresses in each element during the second stage. Thus the internal force vector  $[K] \{x\}$  is modified due to reduction in the value of stiffness [K]. Once again, the elements are scanned for cracking and crushing failure. The cracked elements are replaced and the dynamic analysis is repeated in the third stage. By repeating the above process the cracked and crushed elements are determined. While replacing with cracked elements different values of reduced modulus for concrete such as  $1.0 * E_c$ ,  $0.75 * E_c$ ,  $0.5 * E_c$ ,  $0.25 * E_c$  and  $0.0 * E_c$  have been used to study the effect of tension softening behaviour of concrete and the results are tabulated.

### 3 DISCUSSION OF RESULTS AND CONCLUSION

Figures 4 (a), (b) and (c) shows the El centro (1940) N-S component earthquake input base acceleration and the



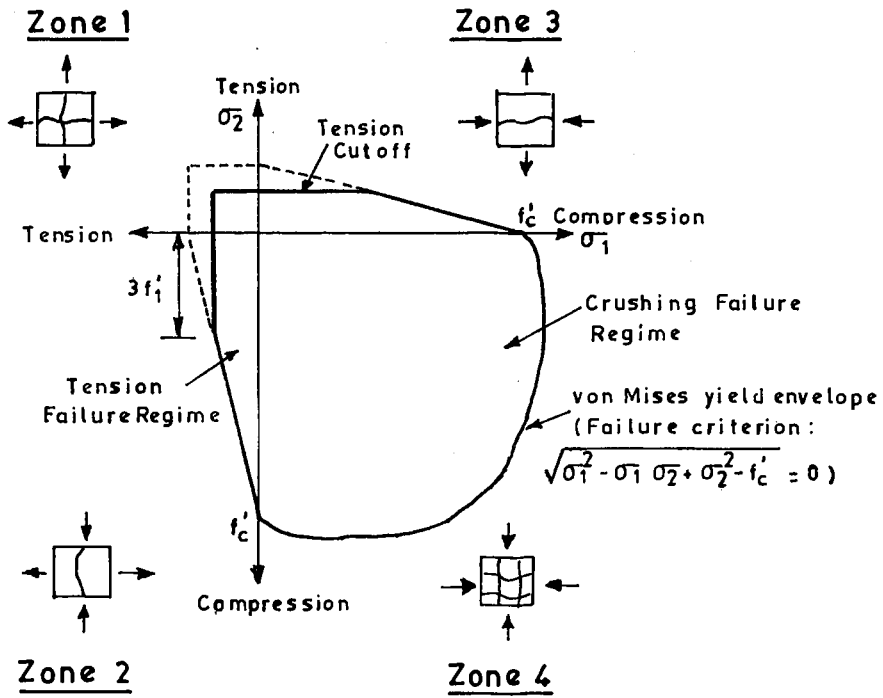


Fig.3(a) - Cracking and Crushing Failure Surfaces of Concrete

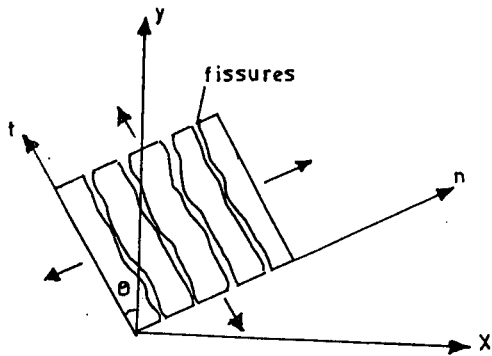


Fig.3(b) - Smeared-Crack Model and Local Coordinates

corresponding time history responses for the horizontal crown displacement at node 1 without and with cracked elements respectively. Table 2 shows the variation in the natural frequencies and period at three stages when the elements are replaced by cracked elements at every stage. Table 3 shows a comparison in the natural frequencies when softening is considered by replacing cracked element with various reduced modulus for concrete. In table 4 the progressive cracked elements and the associated failure zones and the values of maximum and minimum principal stresses for M20 grade of concrete for the three stages are shown. Table 5 shows the tensile crack pattern for considering softening in the dynamic analysis by giving the element number and the associated failure zone numbers. It is observed that the failure in all cases is due to tensile cracks which appears near the junction of the dome and the wall portion of the containment vessel as shown by the element numbers 101, 102, 109, 110, 111, 112, 113, 117, 118, 119 and 120.

Table 2 Natural frequencies at different stages (El centro, 1940, N-S component) for  $E_c = 0.75 * E_c$  for M20 grade of concrete

Mode	First stage		Second stage		Third stage	
	Frequency Hz	Period Sec	Frequency Hz	Period Sec	Frequency Hz	Period Sec
1	5.71	0.1752	5.93	0.1687	6.03	0.1658
2	8.93	0.1120	9.09	0.1101	9.14	0.1095
3	10.26	0.0975	10.80	0.0926	10.81	0.0925
4	11.21	0.0892	11.91	0.0839	11.80	0.0848
5	12.13	0.0825	12.26	0.0815	12.38	0.0808

Table 3 Natural frequencies for various values of Factored  $E_c$  for M20 grade of concrete (El centro, 1940, N-S component) for the degraded structural response

Mode No	$1.0 * E_c$ Frequency Hz	$0.75 * E_c$ Frequency Hz	$0.5 * E_c$ Frequency Hz	$0.25 * E_c$ Frequency Hz	$0.0 * E_c$ Frequency Hz
1	5.71	6.03	6.018	6.005	6.067
2	8.93	9.14	9.122	9.106	9.099
3	10.26	10.81	10.770	10.730	10.680
4	11.21	11.80	11.760	11.730	11.680
5	12.13	12.38	12.350	12.310	12.300

Thus, the present analysis shows most critical failure zone in a nuclear reactor vessel due to tension related fractures, when subjected to earthquake ground motion such as El centro 1940 N-S component as detailed in the present study. Therefore, it is important that the nuclear reactor vessel must be designed as a crack-free structure in order to prevent any nuclear radiation being released which will affect the environment outside in the event of any earthquake ground motion.

Table 4 Progressive cracked element numbers associated failure zone numbers and the values of maximum and minimum principal stresses ( $t/m^2$ ) at different stages for M20 grade of concrete (El centro, 1940, N-S component) ( $E_c = 0.75 * E_c$ )

	I Stage	II Stage	III Stage
Cracked Element Numbers	111,112,113,114 117,118,119,120 8 elements cracked	101,102,109,110 111,112,113,117 118,119,120 11 elements cracked	101,109,110,111 112,113,117,118 119,120 10 elements cracked
Associated Failure Zone Numbers	1,1,2,2,2,2 1,1	1,1,1,1,1,1,1,1 1,1,1	1,1,1,1,1,2,1,1 1,1
Maximum & Minimum Principal stresses in the cracked	312.24,49.33; 291.18,29.64; 254.8,-0.3;205.9 -42.4;205.9,- 42.4;254.8, -0.3;291.2, 29.6;312.2, 49.3	222.5,77.2;210.0, 17.9;209.2,11.2; 222.9,33.5;753.3, 53.7;509.3,91.1; 327.3,77.7;395.7, 77.1;400.5,76.0; 466.8,45.7;533.7, 26.2	384.4,63.2;353.7, 7.4;252.2,23.2; 796.1,24.3;611.4, 59.8;224.1,-6.7; 384.6,77.1;368.9, 69.9;496.0,47.5; 588.6,28.9

Table 5 Tensile crack pattern for various factored values of  $E_c$  showing cracked element numbers and the associated failure zones for M20 grade of concrete (El centro, 1940, N-S component)

Factored values of $E_c$	$1.0 * E_c$	$0.75 * E_c$	$0.5 * E_c$	$0.25 * E_c$	$0.0 * E_c$
Cracked element numbers	111,112, 113,114, 117,118, 119,120 8 elements cracked	101,102, 109,110, 111,112, 113,117, 118,119, 120 11 elements cracked	101,109, 110,111, 112,113, 114,118, 119,120 10 elements cracked	101,109, 110,111, 112,113, 114,117, 118,119, 120 11 elements cracked	101,109, 110,111, 112,114, 117,118, 119,120 10 elements cracked
Associated failure zone numbers	1,1,2,2, 2,2,1,1	1,1,1,1, 1,2,1,1, 1,1	1,1,1,1, 1,2,2,1, 1,1	1,1,1,1, 1,2,2,1, 1,1,1	1,1,1,1, 1,1,1,1, 1,1

## REFERENCES

- Bathe, Edward Wilson, L. and Fred Peterson, E. (1974). SAPIV A structural analysis program for static and dynamic response of linear system, Univ. of California, Berkeley.
- Biggs, John M. (1964). Introduction to Structural Dynamics. Mc Graw Hill Book Co., NY.

- Chang, T.Y., Taniguchi, H. and Chen, W.F. (1987). Nonlinear finite element analysis of reinforced concrete panels, *J. of Structural Engineering*, ASCE, Vol.113, No.1, pp. 122-139.
- Chennakeshava, C. and Sundara Raja Iyengar, K.T. (1988). Elastoplastic cracking analysis of reinforced concrete, *J. of Structural Engineering*, ASCE, Vol.114, No.11, pp.2421-2437.
- Chen, W.F. and Saleeb, A.F. (1982). *Constitutive Equations for Engineering Materials, Vol.1: Elasticity and Modelling*, John Wiley and Sons, NY.
- James Colville and Jamil Abbasi (1974). Plane stress reinforced concrete finite elements, *J. of Structural Engineering*, ASCE, Vol.100, No.ST5, pp. 1067-1083.
- Krishnamoorthy, C.S. and Panneerselvam, A. (1978). FEPACSI - A finite element program for nonlinear analysis of reinforced concrete framed structures, *Computers and Structures*, Vol.9, pp. 451-461.
- Mubbada Suidan, A.M. and William Schnobrich, M. (1973). Finite element analysis of reinforced concrete, *J. of Structural Engineering*, ASCE, Vol.99, No.ST10, pp.2109-2122.
- Ngo, D. and Scordelis, E. (1967). Finite element analysis of reinforced concrete beams, *J. of A.C.I.* 64(3), pp.152-163.
- Nilson, A.H. (1968). Nonlinear analysis of reinforced concrete by the finite element method, *J. of A.C.I.* 65, pp.757-766.
- Raghuprasad, B.K. and Gopalakrishnan, A.R. (1991). Inelastic dynamic analysis of nuclear containment vessels, *SMIRT 11 Transactions*, Vol.H, Tokyo, Japan, pp. 205-210.
- Samannaidu Balakrishnan and David Murray, W. (1988). Concrete constitutive model for NLFE analysis of structures, *J. of Structural Engineering*, ASCE, Vol.114, No.7, pp. 1449-1466.
- Valliappan, S. and Doolan, T.F. (1972). Nonlinear stress analysis of reinforced concrete, *J. of Structural Engineering*, ASCE, Vol.98. No.ST4, pp. 885-897.
- Yew-chaye loo and Yan Yang (1991). Cracking and failure analysis of masonry arch bridges, *J. of Structural Engineering*, ASCE, Vol.117, No.6, pp. 1641-1658.
- Zienkiewicz, O.C., Valliappan, S. and King, I.P. (1969). Elastoplastic solutions of engineering problems 'initial stress' Finite element approach, *Intl. J. for Numerical Methods in Engineering*, Vol.1, pp. 75-100.

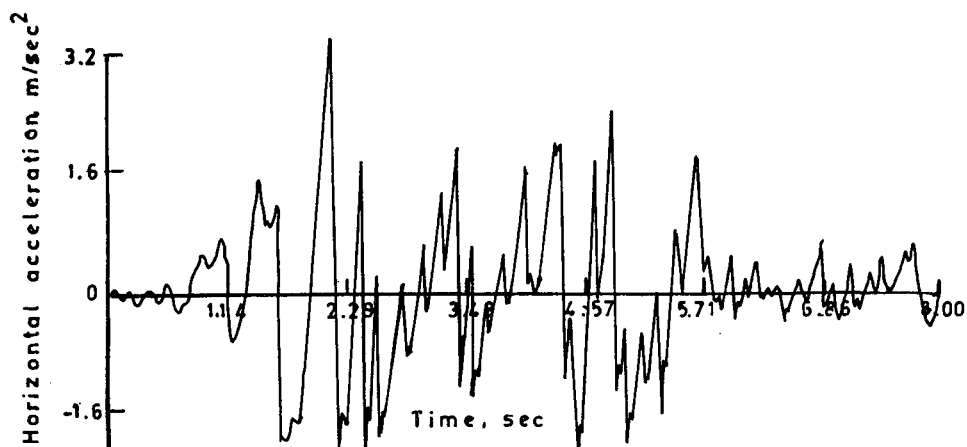


Fig. 4(a)- Elcentro 1940 N-S Component Earthquake input

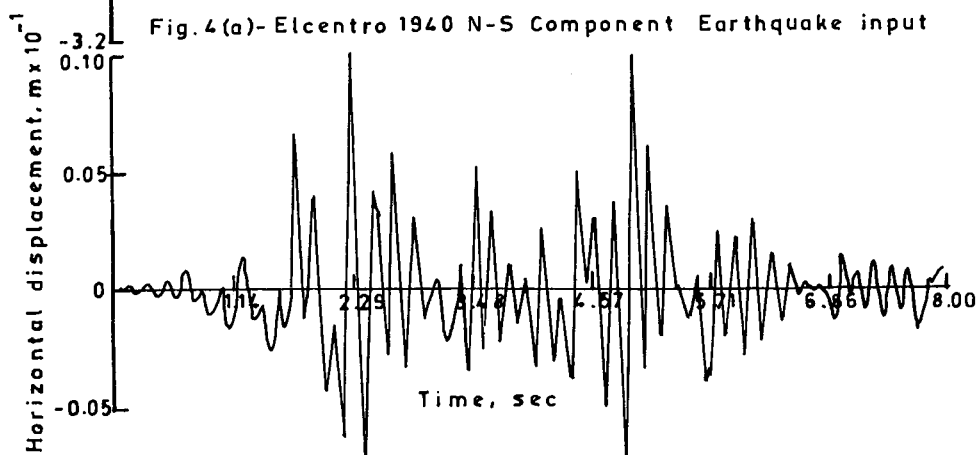


Fig. 4(b) - Crown Displacement Vs. Time with uncracked elements

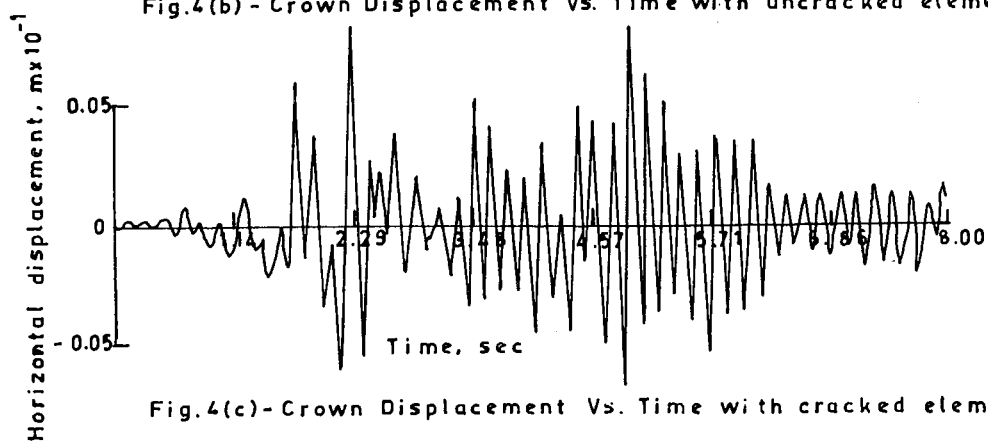


Fig. 4(c) - Crown Displacement Vs. Time with cracked elements

